Syntheses, Solution Properties and Crystal Structures of Peroxo- and Superoxo-Bridged Dinuclear Ammine Rhodium(III) Complexes

Johan Springborg[a,*] and Margareta Zehnder[b]

[a]Chemistry Department, Royal Veterinary and Agricultural University, Thorvaldsensvej 40, DK-1871 Frederiksberg C, Denmark and [b]Institut für Anorganische Chemie der Universität Basel, Spitalstrasse 51, CH-4056 Basel, Switzerland

Springborg, J. and Zehnder, M., 1987. Syntheses, Solution Properties and Crystal Structures of Peroxo- and Superoxo-Bridged Dinuclear Ammine Rhodium(III) Complexes. – Acta Chem. Scand., Ser. A 41: 484–495.

The reaction of $(NH_3)_4Rh(OH)_2Rh(NH_3)_4^{4+}$ with aqueous H_2O_2 at 90 °C forms the μ-hydroxo-μ-peroxo species $(NH_3)_4Rh(OH)(O_2)Rh(NH_3)_4^{3+}$, which was isolated as a pure perchlorate salt (19 %). The peroxo-bridged complex can be oxidized by Ce(IV) to form the corresponding superoxo–bridged complex $(NH_3)_4Rh(OH)(O_2)Rh(NH_3)_4^{4+}$, which was isolated as a pure nitrate salt (91 %). The crystal and molecular structures at room temperature of $[(NH_3)_4Rh(O_2)(OH)Rh(NH_3)_4](ClO_4)_3$ and $[(NH_3)_4Rh(O_2)(OH)Rh(NH_3)_4](NO_3)_4$ have been determined by X-ray diffraction analysis. The crystals of the peroxo compound are monoclinic, space group $P2_1/n$ (No. 14). The lattice constants are: $a = 12.253(2)$, $b = 10.767(2)$, $c = 15.939(5)$ Å and $\beta = 107.17(3)°$. Crystals of the superoxo compound are orthorhombic, space group $Pna2_1$ (No. 33). The lattice constants are: $a = 14.988(3)$, $b = 11.943(3)$ and $c = 10.517(2)$ Å. The dihedral angle of the RhOORh group in the peroxo compound [O–O distance 1.479(8) Å] was found to deviate 62° from planarity, while the superoxo compound [O–O distance 1.337(30) Å] shows no deviation from planarity. The peroxo complex reacts reversibly with acid, and spectrophotometric studies suggest that the reaction involves protonation of the peroxo bridge, with $pK_a = 2.893(5)$ at 25 °C in 1 M $NaClO_4$. A similar reaction was not observed for the superoxo complex for $[H^+] \leq 1.0$ M. The superoxo complex deprotonates in base forming a μ-oxo-μ-superoxo complex, a pK_a value of 14.0(2) (0 °C, 1 M $Na(OH,ClO_4)$) being determined spectrophotometrically. The corresponding pK_a value for the peroxo-bridged complex is significantly higher than 14. The standard reduction potential of the $(NH_3)_4Rh(OH)(O_2)Rh(NH_3)_4^{4+/3+}$ couple was determined potentiometrically to be +0.732 (2) V (vs. SHE; 25 °C, 1 M KNO_3).

Peroxo and superoxo complexes are known for most transition metals. They are of considerable interest because of their relevance to the study of biological processes involving uptake and reduction of dioxygen, and their value as reagents or catalysts in organic chemistry.[1–2] Peroxo and superoxo complexes are very often synthesized by oxidative coordination of dioxygen to low-valent metal complexes. The method has been applied, e.g., to the synthesis of a number of peroxo cobalt(III) complexes.[3] Usually, this method gives binuclear cobalt(III) species, but also mononuclear cobalt(III) species may be formed. An alternative but less common method is the insertion of peroxide by substitution. Recently, we showed that this provides a facile method for the synthesis of rhodium(III) peroxo complexes, which so far have been studied very little.[4–5] It was shown that the Δ,Λ-$(en)_2Rh(OH)_2Rh(en)_2^{4+}$ ion reacts with aqueous H_2O_2 to yield the peroxo-bridged complex Δ,Λ-$(en)_2Rh(OH)(O_2)Rh(en)_2^{3+}$, isolated as a trifluoromethanesulfonate salt (45 %).[5] Furthermore, in our first report on this type of reaction we showed that the corre-

*To whom correspondence should be addressed.

sponding ammine complex reacts similarly but yields several products owing to hydrolysis of ammine ligands.[4] A heptaammine peroxo-bridged complex, *fac*-$[(NH_3)_4Rh(OH)(O_2)Rh(NH_3)_3(H_2O)](ClO_4)_3$, was isolated and this compound as well as its superoxo-bridged analogue were characterized by determination of their X-ray crystal structures.[4] The yields of these heptaammine complexes, however, were rather poor: the peroxo-bridged complex was isolated in a yield of only 2 %. We report here the synthesis and crystal structures of the corresponding octaammine complexes, which have both been crystallized in reasonably good yields using a modification of the methods previously used for the heptaammine complexes.

Experimental

Materials. $[(NH_3)_4Rh(OH)_2Rh(NH_3)_4](ClO_4)_4$ was synthesized as described previously.[6] All other reagents were of analytical grade.

Instruments. A Perkin-Elmer Lambda Diode Array spectrophotometer was used for spectrophotometric measurements. Spectra were recorded with a resolution of 0.25 nm. Data are given with the molar absorption coefficient ε in l mol^{-1} cm^{-1} and the wavelength λ in nm. Electrode potentials were measured using a Radiometer PHM 61 digital voltmeter. Crystal diffraction data were collected with an Enraf-Nonius CAD4 diffractometer equipped with a fine-focus Mo tube and a graphite monochromator to select Mo*K*α radiation.

Analyses. H, N and Cl analyses were performed by the Microanalytical Laboratory at the H. C. Ørsted Institute, Copenhagen.

Preparations. Caution: The solid complex salts described below may *detonate* violently when subjected to mechanical shock. They must therefore be handled with caution and should not be prepared in quantities larger than those described here.

1. *μ-Hydroxo-μ-peroxo-bis[tetraamminerhodium(III)] Perchlorate, $[(NH_3)_4Rh(OH)(O_2)Rh(NH_3)_4](ClO_4)_3$.* A solution of $[(NH_3)_4Rh(OH)_2Rh(NH_3)_4](ClO_4)_4$ (1 g, 1.23 mmol) in 15 % (*w/w*) H_2O_2 (8 ml) was prepared at room temperature. The solution was then heated to 90±1 °C within approximately 15 s and kept at that temperature for 120 s. After approximately 50 s at 90 °C, the colour of the solution began to change from yellow to brown; it became dark brown within the next 30 s and then changed again to yellow at the end of the heating period. During the entire period, a vigorous evolution of gas (O_2) was observed. The mixture was cooled in ice and solid $LiClO_4$ (3 g) was added. The mixture was shaken vigorously in order to dissolve the lithium perchlorate and cooling in ice was continued for a total of 10 min. Yellow crystals of the peroxo complex separated. The crystals were collected and washed three times with 96 % ethanol (3 ml), once with diethyl ether and then dried in the air (0.44 g, 52 %). This crude, rather impure product was purified as follows: The product (0.44 g) was dissolved in water (6 ml) at room temperature and a saturated solution of $NaClO_4$ (1.5 ml) was added to the filtered solution. Yellow crystals separated within minutes. The crystals were collected and washed as above (0.176 g, 40 %). A second recrystallization gave 0.160 g (19 % based on the starting material) of pure $[(NH_3)_4Rh(OH)(O_2)Rh(NH_3)_4](ClO_4)_3$, i.e. the UV spectrum did not change upon further crys-

Table 1. Spectroscopic data for peroxo- and superoxo-bridged dirhodium(III) complexes.

Complex	Medium	$(\varepsilon,\lambda)_{max}$				
$[(NH_3)_4Rh(OH)(O_2)Rh(NH_3)_4](ClO_4)_3$	1 M $NaClO_4$[a]	(4460,286)	(11.000,220)			
–	1 M $HClO_4$[b]	$(418,340)_{sh}$	$(1240,280)_{sh}$	$(7520,210)_{sh}$		
$[(NH_3)_4Rh(OH)(O_2)Rh(NH_3)_4](NO_3)_4$	1 M $NaClO_4$[c]	(69,760)	(1380,503)	(402,390)	(803,318)	$(6710,250)_{sh}$
–	1 M NaOH[d]	(90,760)	(1170,517)	(454,403)	$(744,315)_{sh}$	$(4730,260)_{sh}$

[a] 25 °C; $(\varepsilon,\lambda)_{max}$ = (4510,286) in 1 M NaOH. At 0 °C $(\varepsilon,\lambda)_{max}$ = (4440,286) in 1 M $NaClO_4$. [b] 0 °C and extrapolated back to t_0. [c] 25 °C; $(\varepsilon,\lambda)_{max}$ = (1381,503) in 1 M $HClO_4$. At 0 °C $(\varepsilon,\lambda)_{max}$ = (1402,503) in 1 M $NaClO_4$. [d] 0 °C; these values are nearly identical to those calculated for the μ-oxo-μ-superoxo species shown in Fig. 2.

Table 2. Positional and thermal parameters and their standard deviations for $[(NH_3)_4Rh(OH)(O_2)Rh(NH_3)_4](ClO_4)_3$. The temperature factors are of the form $T = \exp[-2\pi^2(U_{11}h^2a^{*2} + \cdots + 2U_{12}hka^*b^*)]$.

Atom	*x/a*	*y/b*	*z/c*	U_{iso}/Å^2
Rh1	−.1601(1)	−.0931	−.2215	0.0219(5)
Rh2	.0122(1)	−.2553	−.3193	0.0250(5)
O1	−.0164(6)	−.0962(5)	−.2619(5)	0.0349(46)
O2	−.2057(6)	−.2513(1)	−.2863(5)	0.0257(39)
O3	−.1052(5)	−.3335(1)	−.2721(4)	0.0324(46)
N1	−.0742(8)	−.1981(6)	−.1129(6)	0.0360(60)
N2	−.1116(8)	.0750(6)	−.1570(6)	0.0318(54)
N3	−.3104(7)	−.0935(6)	−.1877(7)	0.0278(50)
N4	−.2464(8)	.0096(7)	−.3298(7)	0.0402(66)
N5	−.1125(7)	−.1994(7)	−.4269(6)	0.0405(65)
N6	.1378(8)	−.1698(8)	−.3657(8)	0.0373(60)
N7	.0344(10)	−.4204(7)	−.3748(9)	0.0518(74)
N8	.1363(7)	−.3026(8)	−.2082(7)	0.0501(74)
Cl1	.2134(2)	−.0039(2)	−.0556(2)	0.0429(20)
O10	.1217(9)	.0395(11)	−.0308(9)	0.0740(83)
O11	.3159(9)	.0440(14)	−.0022(7)	0.0839(95)
O12	.2008(12)	.0250(17)	−.1427(7)	0.1012(119)
O13	.2028(16)	−.1375(11)	−.0459(13)	0.1327(150)
Cl2	−.5769(2)	−.0871(2)	−.4021(2)	0.0484(20)
O20	−.3637(10)	−.1412(11)	−.4709(7)	0.0906(100)
O21	−.6103(9)	−.0852(7)	−.3228(7)	0.0547(61)
O22	−.4710(9)	−.1542(9)	−.6873(8)	0.0782(87)
O23	−.5589(11)	.0357(7)	−.4259(8)	0.0691(77)
Cl3	.0160(2)	.1766(2)	−.3749(2)	0.0391(18)
O30	.0298(12)	.2905(8)	−.4133(8)	0.1083(117)
O31	.1156(10)	.1166(11)	−.3466(15)	0.0689(80)
O32	.0476(10)	−.1887(7)	−.6839(8)	0.0622(71)
O33	.0506(17)	−.0893(10)	−.5577(8)	0.1178(130)
H10	−.0193(8)	−.1450(6)	−.0595(6)	0.0500
H11	−.0239(8)	−.2661(6)	−.1350(6)	0.0500
H12	−.1386(8)	−.2449(6)	−.0907(6)	0.0500
H20	−.0676(8)	.0651(6)	−.0879(6)	0.0500
H21	−.1837(8)	.1365(6)	−.1657(6)	0.0500
H22	−.0538(8)	.1131(6)	−.1900(6)	0.0500
H30	−.2888(7)	−.1312(5)	−.1220(7)	0.0500
H31	−.3750(7)	−.1508(6)	−.2313(7)	0.0500
H32	−.3423(7)	−.0002(6)	−.1876(7)	0.0500
H40	−.1791(8)	.0117(7)	−.3607(7)	0.0500
H41	−.2635(8)	.1014(7)	−.3094(7)	0.0500
H42	−.3228(8)	−.0271(7)	−.3757(7)	0.0500
H50	−.1055(7)	−.2614(7)	−.4783(6)	0.0500
H51	−.0857(7)	−.1074(7)	−.4391(6)	0.0500
H52	−.2002(7)	−.1965(7)	−.4258(6)	0.0500
H60	.1004(8)	−.1360(8)	−.4318(8)	0.0500
H61	.1928(8)	−.2478(8)	−.3668(8)	0.0500
H62	.1872(8)	−.0966(8)	−.3257(8)	0.0500
H70	.1025(10)	−.3959(7)	−.4020(9)	0.0500
H71	−.0433(10)	−.4352(7)	−.4275(9)	0.0500
H72	.0568(10)	−.5044(7)	−.3366(9)	0.0500
H80	.2084(7)	−.2690(8)	−.2275(7)	0.0500
H81	.1406(7)	−.4026(8)	−.2028(7)	0.0500
H82	.1682(7)	−.2629(8)	−.1456(7)	0.0500

tallization. Anal. $Rh_2N_8H_{25}O_{15}Cl_3$: H, N, Cl. Spectral data are given in Table 1 and spectra are shown in Fig. 1. Crystals for the X-ray structure analysis were obtained as described for the recrystallization above, but using less $NaClO_4$.

2. *μ-Hydroxo-μ-superoxo-bis(tetraamminerhodium(III)) nitrate, $[(NH_3)_4Rh(OH)(O_2)Rh(NH_3)_4](NO_3)_4$.* To a solution of the peroxo complex salt, $[(NH_3)_4Rh(OH)(O_2)Rh(NH_3)_4](ClO_4)_3$ (0.5 g, 0.73 mmol), in water (10 ml) was added 0.42 M HNO_3, 0.42 M $(NH_4)_2Ce(NO_3)_6$ at room temperature. The colour of the solution changed instantaneously from yellow to red. After 15 s, a saturated solution of $NaNO_3$ (5 ml) was added and red crystals of the superoxo complex precipitated. The crystals were collected after 2 min, washed twice with 4 M HNO_3 (3 ml), three times with 96 % ethanol (5 ml), and finally with diethyl ether. The product was dried in the air (0.42 g, 91 %). A sample (0.1 g) was dissolved in water (5 ml) at room temperature and a saturated solution of $NaNO_3$ (2 ml) was then added to the filtered solution. The crystals were isolated as above (0.075 g, 75 %). The VIS–UV spectrum of the product did not change upon further recrystallization. Anal. $Rh_2N_{12}H_{25}O_{15}$: H, N. Spectral data are given in Table 1 and spectra are shown in Fig. 2. Crystals for the X-ray structure analysis were obtained as described for the recrystallization above, but using less $NaNO_3$.

Determination of pK_a for the μ-hydrogenperoxo-μ-hydroxorhodium(III) cation. The acid dissociation constant, K_a, for the hydrogenperoxo-bridged cation, $(NH_3)_4Rh(HO_2)(OH)Rh(NH_3)_4^{4+}$, was determined from spectroscopic measurements on solutions of $[(NH_3)_4Rh(OH)(O_2)Rh(NH_3)_4](ClO_4)_3$ in 1 M $(Na,H)ClO_4$ at 1.5 °C and 25.0 °C. The reversibility of the reaction with acid was shown as follows: A 3×10^{-4} M solution of $[(NH_3)_4Rh(OH)(O_2)Rh(NH_3)_4](ClO_4)_3$ in 0.1 M $HClO_4$, 0.9 M $NaClO_4$ was kept at 0 °C for 20 s and was then mixed with an equal volume of ice-cold 0.2 M NaOH, 0.9 M $NaClO_4$. The UV spectrum of this solution showed $(\varepsilon,\lambda)_{max}$ = (4473,286), which is nearly the same as found for $[(NH_3)_4Rh(OH)(O_2)Rh(NH_3)_4](ClO_4)_3$ in neutral or basic solution (Table 1). A similar result was obtained when base was added to the acidic solution after 40 s.

The spectra of acidic solutions of $[(NH_3)_4Rh(OH)(O_2)Rh(NH_3)_4](ClO_4)_3$ changed with time, and the molar absorption coefficients at the time of dissolution, ε_o, were therefore obtained by linear extrapolations based on 2–3 absorption curves recorded within 1–4 min after dissolution. Such extrapolation led to a correction of about 1 % at 1.5 °C and 4 % at 25.0 °C.

Spectral data for solutions with $[H^+]$ = 0.2 and 1.0 M were identical and were therefore assumed to correspond to the pure protonated species. Spectral data for the deprotonated species were obtained from measurements in 1 M $NaClO_4$. The acid dissociation constant was then obtained by least-squares calculations, using ε_o-values, at λ = 280, 290, 300 and 310 nm, measured on solutions with C_{HClO_4} = 0.0005, 0.001, 0.002, 0.005, 0.01 and 0.1 M, and with $C_{dinuclear} \sim 2\times10^{-4}$ M. This gave $K_a = 7.32(9)\times10^{-4}$ M at 1.5 °C and $K_a = 1.280(15)\times10^{-3}$ M at 25.0 °C.

Determination of the acid dissociation constant for the μ-hydroxo-μ-superoxo rhodium(III) cation. The reversibility of the reaction of the μ-hydroxo-μ-superoxo complex with base was shown as follows: An 8×10^{-4} M solution of $[(NH_3)_4Rh(OH)(O_2)Rh(NH_3)_4](NO_3)_4$ in 0.1 M NaOH was kept at 0 °C for 7 s and then mixed with an equal volume of ice-cold 0.2 M $HClO_4$, 1.8 M $NaClO_4$. The spectrum of this solution showed $(\varepsilon,\lambda)_{max}$ = (1412,502), which is the same as found for $[(NH_3)_4Rh(OH)(O_2)Rh(NH_3)_4](NO_3)_4$ in neutral or acidic solution (Table 1). The base dissociation constant, K_b, was determined from spectroscopic measurements on 4×10^{-4} M solutions of the nitrate salt in 1 M $NaClO_4$ and in 1 M Na(ClO_4,OH) with $[OH^-]$ = 0.01, 0.05, 0.1, 0.2, 0.5 and 1.0 M at 0 °C. K_b was then determined by least-squares calculation using molar absorption coefficients measured at 30 wavelengths in the region 440–620 nm. This gave K_b = 0.20(7) M and, using pK_w = 14.72, pK_a = 14.0(2). K_b was then used to calculate the spectrum of the μ-oxo-μ-superoxo species (Table 1, Fig. 2).

Kinetic measurements. Kinetic data for the oxidation of the peroxo complex by $S_2O_8^{2-}$ and for the decomposition of the peroxo complex in acidic solution were obtained from spectrophotometric measurements at λ = 500 nm. For both reactions, the change of absorbance with time followed

Table 3. Positional and thermal parameters and their standard deviations for $[(NH_3)_4Rh(OH)(O_2)Rh(NH_3)_4](NO_3)_4$. The temperature factors are of the form $T = \exp[-2\pi^2(U_{11}h^2a^{*2} + \cdots + 2U_{12}hka^*b^*)]$.

Atom	*x/a*	*y/b*	*z/c*	U_{iso}/Å^2
Rh1	.1266(1)	.2059(2)	.2500	0.0224(14)
Rh2	.1264(1)	.2060(2)	.5750(1)	0.0237(15)
O1	.1675(5)	.2842(5)	.4149(25)	0.0285(48)
O2	.0544(12)	.0967(15)	.3519(19)	0.0368(102)
O3	.0532(13)	.0950(14)	.4789(21)	0.0232(74)
N1	.0203(13)	.3125(18)	.2336(21)	0.0150(71)
N2	.2040(18)	.3120(22)	.1339(22)	0.0334(113)
N3	.0861(17)	.1255(22)	.0933(22)	0.0539(137)
N4	.2396(15)	.1039(20)	.2629(22)	0.0163(73)
N5	.0092(16)	.3052(17)	.5960(25)	0.0530(107)
N6	.2009(13)	.3208(22)	.6739(20)	0.0295(95)
N7	.0899(21)	.1166(22)	.7413(25)	0.0218(80)
N8	.2382(16)	.1064(20)	.5743(27)	0.0507(131)
N10	.4281(6)	−.0693(8)	.4238(24)	0.0306(60)
O10	.4242(6)	−.1732(7)	.4123(26)	0.0456(55)
O11	.4389(12)	−.0229(17)	.3099(20)	0.0522(102)
O12	.4192(10)	−.0162(12)	.5141(15)	0.0430(84)
N20	.1313(7)	−.1401(8)	.3885(11)	0.0360(77)
O20	.1074(9)	−.1433(12)	.2814(14)	0.0596(100)
O21	.0876(11)	−.1740(13)	.4852(17)	0.0585(87)
O22	.2062(5)	−.0936(6)	.4247(15)	0.0365(46)
N30	.1422(6)	−.1504(8)	−.0701(14)	0.0329(69)
O30	.1283(6)	−.2504(7)	−.1079(10)	0.0361(60)
O31	.1383(8)	−.1231(10)	.0419(12)	0.0495(76)
O32	.1615(8)	−.0802(10)	−.1536(12)	0.0598(90)
N40	.3095(6)	.0705(8)	−.0974(18)	0.0349(57)
O40	.3418(13)	.0367(17)	−.1967(19)	0.0471(93)
O41	.3307(14)	.0242(17)	.0104(20)	0.0517(99)
O42	.2568(5)	.1496(7)	−.0739(17)	0.0447(63)
H10	.0151	.3875	.1753	0.0500
H11	.0103	.3194	.3240	0.0500
H12	−.0339	.2536	.1878	0.0500
H20	.1831	.3620	.0572	0.0500
H21	.2307	.2374	.1162	0.0500
H22	.2510	.3657	.1941	0.0500
H30	.1354	.1370	.0125	0.0500
H31	.0213	.1428	.0527	0.0500
H32	.0894	.0358	.1154	0.0500
H40	.2196	.0317	.3137	0.0500
H41	.2832	.1559	.3153	0.0500
H42	.2743	.0767	.1743	0.0500
H50	.0559	.3570	.6494	0.0500
H51	−.0481	.2885	.6385	0.0500
H52	−.0058	.3630	.5068	0.0500
H60	.1585	.3881	.6647	0.0500
H61	.2562	.3196	.6127	0.0500
H62	.2263	.3163	.7749	0.0500
H70	.0316	.1651	.7631	0.0500
H71	.1356	.1127	.8142	0.0500
H72	.0707	.0355	.7052	0.0500
H80	.2213	.0226	.5428	0.0500
H81	.2484	.1129	.6697	0.0500
H82	.2977	.1330	.5191	0.0500

pseudo first-order kinetics for at least four half-lives, and spectra recorded at $t = 6\times t_{\frac{1}{2}}$ and $t = 7\times t_{\frac{1}{2}}$ were identical.

The spectra of the product solutions for the reactions with $S_2O_8^{2-}$ were identical with that of the μ-hydroxo-μ-superoxo complex shown for the region λ = 800–400 nm.

For the decomposition (disproportionation) reactions in acid, the spectra of the product solutions in the region 800–400 nm were consistent with formation of the μ-hydroxo-μ-superoxo complex together with products which do not absorb in this region. The yield of the superoxo complex formed was calculated from the absorbance at 500 nm, assuming that no other products absorb significantly at this wavelength.

Redox potential. The standard redox potential of the $(NH_3)_4Rh(OH)(O_2)Rh(NH_3)_4^{4+/3+}$ couple was determined potentiometrically using a Pt electrode and calomel reference electrode: The potential of the reference electrode was determined relative to a quinhydrone electrode at pH = 4.008 (phthalate buffer) and pH = 6.865 (phosphate buffer) at 25 °C, giving a value of 245.3(15) mV.[7] The standard redox potential of the peroxo/superoxo systems was then determined from the potentials of solutions of mixtures of $[(NH_3)_4Rh(OH)(O_2)Rh(NH_3)_4](ClO_4)_3$ and $[(NH_3)_4Rh(OH)(O_2)Rh(NH_3)_4](NO_3)_4$ in 1 M KNO_3. Stable readings were obtained within seconds. A total of 11 determinations with $C_{dinuclear} \approx 10^{-3}$ M and [red]/[ox] varying from 0.25 to 4.0 was made. This gave E° = 731.5(15) mV. No corrections for liquid-junction potentials were made.

Crystal data and structure determinations. Crystal data for the peroxo compound ($Rh_2Cl_3O_{15}N_8H_{25}$) are: monoclinic, space group $P2_1/n$, a = 12.253(2), b = 10.767(2), c = 15.939(5) Å, β = 107.17(2)°, D_{obs} = 2.28, D_{calc} = 2.2279 g cm^{-3} for Z = 4; U = 2009.1(2) Å^3, $F(000)$ = 1368. Crystal data for the superoxo compound are: orthorhombic, space group $Pna2_1$, a = 14.988(3), b = 11.943(3), c = 10.517(2) Å, D_{obs} = 2.26, D_{calc} = 2.255 g cm^{-3} for Z = 4; U = 1882.56(3) Å^3, $F(000)$ = 1276.

Single crystals of the compounds were mounted in 0.3 mm Lindemann capillaries. Intensities and cell dimensions were determined on an Enraf-Nonius CAD4 diffractometer using graphite-monochromated Mo$K\alpha$ radiation. The θ-values of 25 strong, independent reflections were used to refine the cell parameters by the least-squares method. Intensity data were collected at room temperature using the θ/2θ scan mode. The scanning speed was varied according to the intensity (0.02–0.50° sec.$^{-1}$). For the peroxo compound, the reciprocal space was explored in the octants *hkl and h −k l from* θ = 3° to θ = 25°, yielding 4690 independent reflections. For the superoxo compound, the reciprocal space was explored in the octant *hk −l from* θ = 2° to θ = 25°, yielding 2265 independent reflections. Four standard reflections monitored every 3600 s for both structures showed no intensity loss. The intensities were corrected for polarization and Lorentz effects, but not for absorption.

The structures were solved by the Patterson technique. In the superoxo compound (space group $Pna2_1$) the z positional parameter for one of the two metal centres was held fixed. Differ-

Table 4. Bond distances (Å) and selected bond angles (°).

	Peroxo compound	Superoxo compound
Distances		
O(2)–O(3)	1.479(8)	1.337(30)
Rh(1)–O(1)	2.045(8)	2.064(23)
Rh(1)–O(2)	1.984(5)	2.005(19)
Rh(1)–N(1)	2.076(3)	2.046(20)
Rh(1)–N(2)	2.080(7)	2.108(26)
Rh(1)–N(3)	2.066(10)	2.002(24)
Rh(1)–N(4)	2.060(9)	2.090(23)
Rh(2)–O(1)	2.021(6)	2.021(23)
Rh(2)–O(3)	1.996(7)	1.995(20)
Rh(2)–N(5)	2.023(8)	2.131(21)
Rh(2)–N(6)	2.106(11)	2.052(23)
Rh(2)–N(7)	2.039(10)	2.121(27)
Rh(2)–N(8)	2.028(9)	2.054(24)
Angles		
Rh(1)–O(1)–Rh(2)	115.9(3)	113.6(4)
Rh(1)–O(2)–O(3)	109.9(4)	123.5(14)
Rh(2)–O(3)–O(2)	110.5(4)	119.2(14)
O(1)–Rh(1)–N(1)	88.9(3)	91.1(7)
O(1)–Rh(1)–O(2)	87.6(3)	90.3(7)
O(2)–Rh(1)–N(4)	91.7(3)	91.4(8)
O(1)–Rh(2)–N(5)	86.7(3)	94.6(7)
O(1)–Rh(2)–O(3)	86.9(3)	93.1(8)
O(3)–Rh(2)–N(8)	90.2(3)	93.6(9)
Rh(1)–O(2)–O(3)–Rh(2)	62	0.0

ence Fourier maps and subsequent least-squares refinements located all non-hydrogen atoms. Anisotropic blocked-matrix least-squares refinements using 2137 reflections for the peroxo compound [$F_o > 2\sigma(F_o)$] and 1863 reflections for the superoxo compound [$F_o > 1\sigma(F_o)$], and introducing H atoms localized from final ΔF maps and refined isotropically, gave R-values of 0.0494 and 0.0447, respectively ($R = \Sigma||F_o|-|F_c||/|F_o|$). The refinements were stopped when Δ/σ was less than 0.1 for all non-hydrogen atoms. Final weighting of the form $w = [\sigma^2(2F_o) + g(F_o)^2]^{-1}$ was used, where g was 0.0440 for the peroxo compound, leading to a final R-value of 0.0468, and 0.00458 for the superoxo compound, leading to a final R-value of 0.0497. Tables 2 and 3 summarize positional and thermal parameters, and Table 4 gives a selection of relevant bond distances and bond angles. A list of observed and calculated structure factors as well as anisotropic temperature factors is available from the authors upon request.

Programs used were those of Sheldrick.[8] Scattering factors for Rh^{3+} and neutral atoms were taken from Cromer *et al.*,[9,10] except those for H atoms, which are from Stewart *et al.*[11]

Results and discussion

Formation of the peroxo complex. Heating a solution of $[(NH_3)_4Rh(OH)_2Rh(NH_3)_4](ClO_4)_4$ in aqueous H_2O_2 (15 %) at 90 °C led to formation of the peroxo-bridged cation **2** [eqn. (1)]:

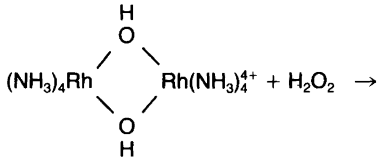

1

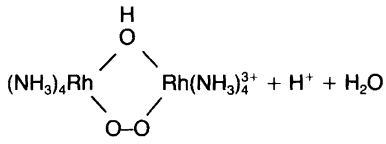

(1)

2

In the reaction between **1** and H_2O_2 the colour gradually changed from yellow to brown during the first 80 s. Within the same period a vigorous evolution of oxygen was observed. The colour then changed again to yellow at the end of the heating period. Subsequent further addition of H_2O_2 did not lead to a similar (vigorous) evolution of oxygen. The disproportionation of H_2O_2 to H_2O and O_2 seems to be associated with the formation of the strongly coloured intermediates, but the nature of these is at present unknown.

The reaction in eqn. (1) is seen to produce acid, but the reaction mixture becomes slightly basic (pH 8) during the reaction. This is explained by subsequent hydrolysis of coordinated ammonia, leading to a heptaamminedirhodium complex [eqn. (2)] together with other unidentified products. The isolation (in very low yield) of the perchlorate salt of **3** and the determination of its crystal structure has been reported previously.[4] The hydrolysis reaction [eqn. (2)] takes

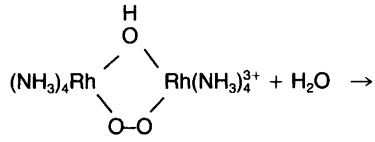

2

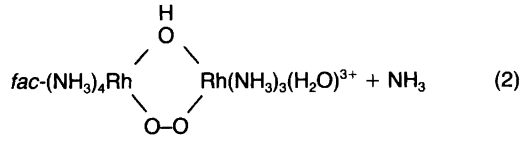

(2)

3

place on the same time scale as the reaction with H_2O_2 [eqn. (1)], and thereby prohibits the formation of a large yield of **2**. A reaction time of 2 min at 90 °C was found to give a maximum yield of **2**, which was isolated as a perchlorate salt. The crude, rather impure product (yield 52 %) had to be recrystallized twice before it was pure (total yield 19 %). Addition of base (NH_3 or NaOH) or lowering of the reaction temperature (60 °C) was found not to improve the yield of the pure product. The crystal structure of the perchlorate of **2** is described below.

Formation of the superoxo complex. Oxidation of the μ-hydroxo-μ-peroxo complex by Ce(IV) leads to the corresponding red μ-hydroxo-μ-superoxo complex [eqn. (3)], which was isolated as

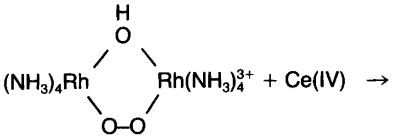

2

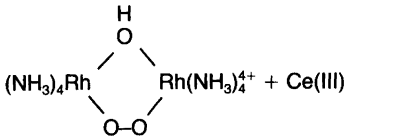

(3)

4

a red-brown nitrate salt (yield 91 %). The crystal structure of this salt is described below. The reaction with Ce(IV) is quantitative (>99 %), as shown spectrophotometrically, and very fast ($t_{\frac{1}{2}} <$ 1 s for [Ce(IV)] = 5×10^{-2} M and [Rh] = 10^{-3} M).

Likewise, peroxodisulfate is capable of oxidizing the peroxo complex to its superoxo analogue. This reaction is also essentially quantitative (>97 %), and for high concentrations of $S_2O_8^{2-}$ it is first-order with respect to the peroxo complex. For 1.0 M $Na_2S_2O_8$ the value $k_{obs} = 5.3\times10^{-3}$ s^{-1} was obtained at 25 °C. The kinetics of this reaction are presently being studied further.

The superoxo-bridged complex may also be formed by a disproportionation reaction of **2** in acidic solution. The yield of superoxo complex was found to depend on the concentration of the rhodium(III) complex. For 8×10^{-5} M and 3×10^{-3} M solutions of the peroxo complex in 1 M $HClO_4$ (25 °C), the yield of the superoxo complex was found to be 26 % and 36 %, respectively [based upon total Rh(III)]. These yields are significantly smaller than the yield of 67 % calculated on the basis of eqn. (4). Since the superoxo complex is stable under the experimental conditions, it is therefore clear that other reactions compete with the disproportionation reaction [eqn. (4)], and the product distribution is therefore more complicated than expressed by eqn. (4). The disproportionation (monitored at λ = 500 nm) followed first-order kinetics for at least three half-lives. Furthermore, the same rate constants were obtained for solutions with $C_{Rh} = 6\times10^{-3}$ M and 2×10^{-4} M, which gave $k = 7.3(7)\times10^{-4}$ s^{-1} (25 °C, 1 M $HClO_4$).

On the basis of the present studies it cannot be established whether the disproportionation involves direct redox reactions between two peroxo complexes or hydrolysis of peroxide with subsequent redox reaction between released H_2O_2 and **2**. The fact, however, that the formation of the superoxo complex is first-order with respect to the peroxo complex seems to indicate that neither of these bimolecular reactions are rate-determining steps. Similar disproportionation reactions have been reported for μ-peroxo dicobalt (III) complexes; the mechanism of these reactions is, however, not known.[3] Halide ion catalyzed disproportionation of the dicobalt(III) complexes has also been reported.[3]

The standard reduction potential of the $(NH_3)_4Rh(OH)(O_2)Rh(NH_3)_4^{4+/3+}$ couple was determined potentiometrically to be $E^\circ = 0.732(2)$ V (25 °C, 1 M KNO_3). This is significantly smaller than values reported for corresponding amine cobalt(III) systems (0.9–1.1 V).[12]

Spectra and acid-base equilibria. The acid-base properties of the two complexes were studied spectrophotometrically.

The peroxo complex reacts reversibly with acid. The spectra of solutions of the peroxo complex in acid changed with time and extrapolations back to the time of dissolution were therefore required. By analogy with our previous study of the ethylenediamine analogue, this reaction is interpreted as a protonation of the peroxo bridge, as shown in eqn. (5).

From spectrophotometric measurements in the [H$^+$] region 10^{-5} – 1.0 M at two temperatures (1.5 °C and 25.0 °C), the acid dissociation con-

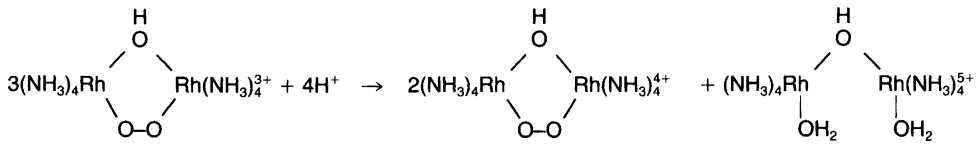

(4)

2 **4** **5**

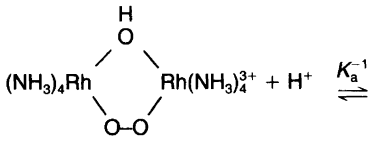

2

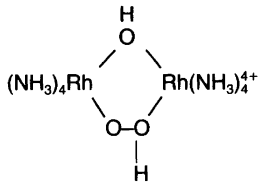

6 (5)

stant in eqn. (5) was determined as pK_a = 2.893(5) at 25 °C with ΔH° = 16.2(4) kJ mol^{-1} and $\Delta S^\circ = -1(1)$ J mol^{-1} K^{-1}. The spectral data for the two species are given in Table 1 and spectra are shown in Fig. 1. Owing to the instability of the μ-hydrogenperoxo-μ-hydroxo complex in aqueous solution, attempts to crystallize salts of this cation have so far been unsuccessful.

Our previously reported[5] values for the ethylenediamine analogue, Δ,Λ-$(en)_2Rh(OH)(HO_2)Rh(en)_2^{4+}$, are pK_a = 2.70(2), ΔH° = 14.8(16) kJ mol^{-1} and $\Delta S^\circ = -2(6)$ J mol^{-1} K^{-1}. These values are very close to those for the present ammine system, which is a reasonable result since the non-bridging ligands are similar.

The superoxo-bridged complex is stable for hours in acidic (1 M $HClO_4$) and neutral solutions. The fact that the spectra in 1 M $NaClO_4$ and in 1 M $HClO_4$ are identical implies that protonation of the superoxo bridge does not occur. The μ-hydrogensuperoxo-μ-hydroxo complex must therefore be a strong acid with $K_a \gg 1$ M. It can be seen that the difference in acid strength of bridging HO_2 and HO_2^- ($pK_a < 0$ and pK_a = 2.9, respectively) qualitatively parallels the observed difference for the free ligands (HO_2: pK_a = 4.7; HO_2^-: $pK_a \approx 16$).[13,14] The difference in kinetic stability of the μ-superoxo and μ-peroxo com-

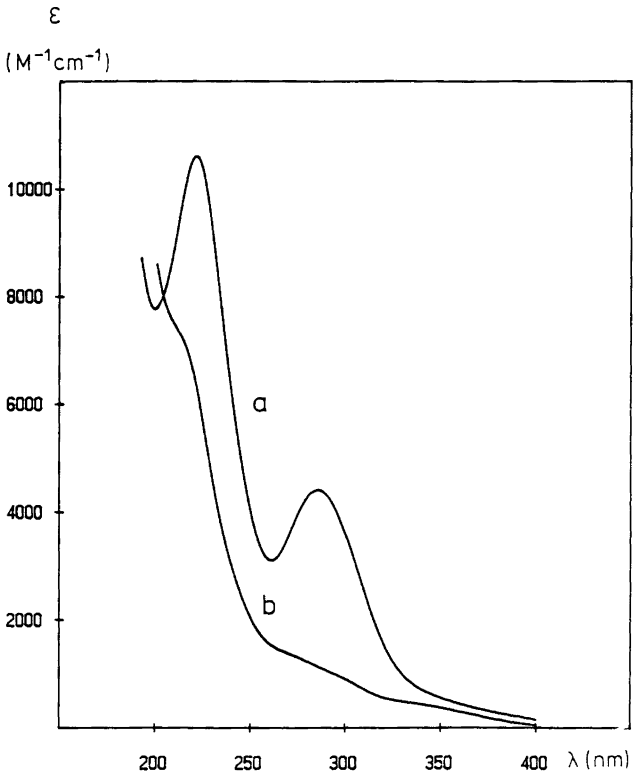

Fig. 1. Absorption spectra of the μ-hydroxo-μ-peroxo complex **2** (curve a) and the μ-hydrogenperoxo-μ-hydroxo complex **6** (curve b) recorded at 1.5 °C in 1.0 M $(Na,H)ClO_4$.

plexes in acidic solution may be related to the difference in acid strength of the corresponding protonated species.

The colour of neutral aqueous solutions of the μ-hydroxo-μ-superoxo complex changes instantaneously from red to reddish-purple when strong base is added. The reaction giving this colour shift is reversible, as shown spectrophotometrically. Since fast reversible reactions are not likely to involve Rh–O bond cleavage or bond formation, the reaction is interpreted as an acid-base equilibrium involving deprotonation of the hydroxo bridge [eqn. (6)].

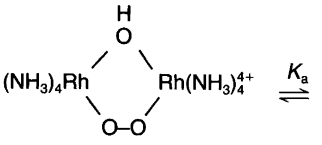

4

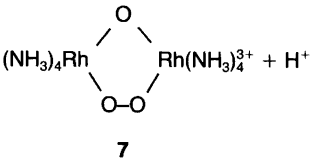

7 (6)

The spectra in base changed with time and extrapolation back to the time of dissolution was therefore necessary. From spectrophotometric measurements on solutions with $[OH^-] = 10^{-7}$ – 1.0 M, the acid dissociation constant in eqn. (6) was determined as $pK_a = 14.0(2)$ (0 °C, I = 1.0 M). The spectrum of the μ-hydroxo-μ-superoxo species (1 M $NaClO_4$) and the calculated spectrum of the μ-oxo-μ-superoxo species are shown in Fig. 2 (see also Table 1). Similar spectroscopic studies of the μ-hydroxo-μ-peroxo complex showed that this complex does not deprotonate in 1 M NaOH and therefore has $pK_a > 14$ (Table 1). The observation that the μ-hydroxo-μ-superoxo complex is a stronger acid than the μ-hydroxo-μ-peroxo complex is qualitatively in keeping with the behaviour expected on the basis of the different charges of the two acids. The

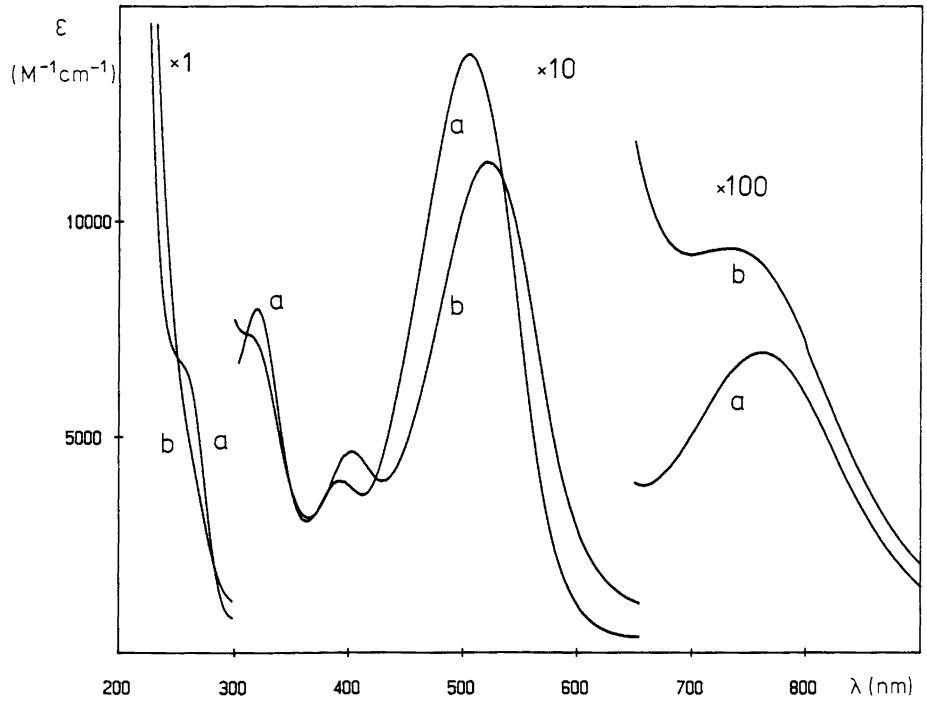

Fig. 2. Absorption spectra of the μ-hydroxo-μ-superoxo complex **4** (curve a) recorded at 0 °C in 1 M $NaClO_4$, and the calculated spectrum of the μ-oxo-μ-superoxo complex **7** (curve b).

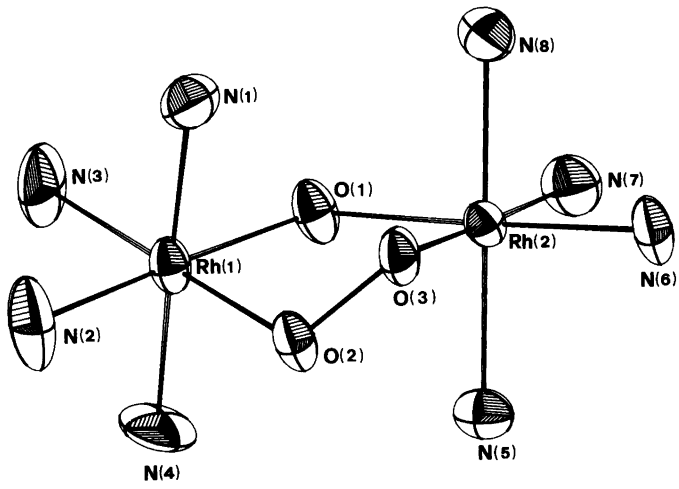

Fig. 3. ORTEP drawing of the peroxo complex, $(NH_3)_4Rh(OH)(O_2)Rh(NH_3)_4^{3+}$.

stabilities of the peroxo and superoxo species in basic solution are also quite different. The spectrum of a solution of the peroxo complex in 1 M NaOH at 25 °C remained unchanged for at least 10 min. In contrast, a solution of the superoxo complex in 1 M NaOH at 25 °C changed colour from red to yellow within 3–4 min. The nature of this reaction is presently being studied.

Finally, it is noted that the VIS–UV spectra of the present peroxo- and superoxo-bridged dirhodium(III) complexes show many features which are similar to those reported for analogous dicobalt(III) species. A rather detailed discussion of the electronic and spectral properties of the dicobalt(III) complexes has been given recently.[15–17]

Description of the structures. The asymmetric units in the peroxo compound and in the superoxo compound contain one discrete binuclear complex cation and three and four anions, respectively. Figs. 3 and 4 show ORTEP drawings of the cations. The O(2)–O(3) distance of 1.479(8) Å in the peroxo compound is close to that found for the corresponding ethylenediamine compound [1.521(14) Å] and almost identical to that in the aquaheptaammine compound [1.489(23) Å]. The Rh(1)–O(2)–O(3)–Rh(2) unit is non-planar, as found in all previously determined structures of dinuclear μ-peroxo-μ-hydroxo complexes, and the dihedral angle is 62°, which is close to the values observed for the corresponding ethylenediamine and aquaheptaammine complexes [62.8(5) and 62.2(5)°, respectively]. The coordination octahedra are distorted;

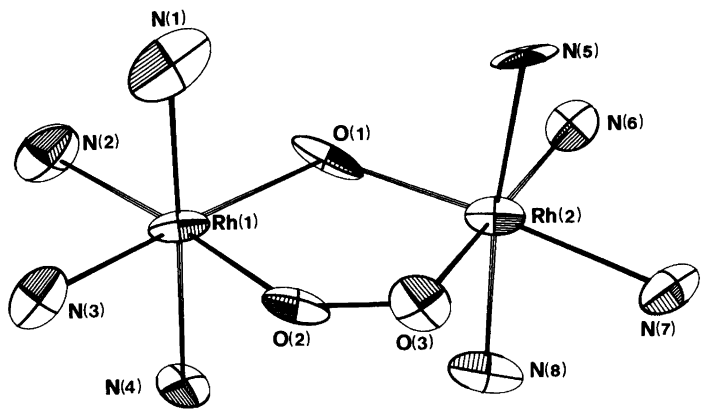

Fig. 4. ORTEP drawing of the superoxo complex, $(NH_3)_4Rh(OH)(O_2)Rh(NH_3)_4^{4+}$.

bond angles range from 87° to 93° and bond distances are in the range 1.99 Å–2.08 Å.

The O(2)–O(3) distance of 1.337(30) Å in the superoxo compound is close to the distance [1.322(18) Å] found in the corresponding aquaheptaammine complex. The Rh(1)–O(2)–O(3)–Rh(2) unit is planar. In contrast, the two superoxo-bridged complexes *fac*-$(H_2O)(NH_3)_3Rh(OH)(O_2)Rh(NH_3)_4^{4+}$ and $\Delta,\Delta/\Lambda,\Lambda$-$(en)_2Co(OH)(O_2)Co(en)_2^{4+}$ have a non-planar MOOM unit with dihedral angles of 7.1 and 22.0°, respectively.[4,18] The coordination octahedra are distorted, bond angles ranging from 88° to 94° and bond distances being in the range 1.94 Å–2.14 Å.

The Rh(1)–O(1)–Rh(2) angles in the peroxo and superoxo compounds are similar [115.9(3)° and 113.6(4)°, respectively] and significantly larger than the Rh–O–Rh angles of 100.5(3)° reported for *trans*-$(H_2O)(tacn)Rh(OH)_2Rh(tacn)(H_2O)^{4+}$ (tacn = 1,4,7-triazacyclononane).

Acknowledgements. Financial support by the Carlsberg Foundation, the Danish Natural Science Research Council, by the Swiss National Science Foundation (grant 2.42–0.79), and by the *Ciba Geigy Stiftung,* Basle, is gratefully acknowledged. We thank Dr. Martin Hancock for valuable comments.

References

1. Hanzlik, R. P. *Inorganic Aspects of Biological and Organic Chemistry,* Academic Press, New York 1976.
2. Sheldon, R. A. and Kochi, J. K. *Metal Catalyzed Oxidations of Organic Compounds,* Academic Press, New York 1981.
3. Fallab, S. and Mitchell, P. R. In: Sykes, A. G., Ed., *Adv. Inorg. Bioinorg. Mechanisms,* Academic Press 1984, Vol. 3, p. 311.
4. Springborg, J. and Zehnder, M. *Helv. Chim. Acta 67* (1984) 2218.
5. Springborg, J. and Zehnder, M. *Helv. Chim. Acta 69* (1986) 199.
6. Christensson, F. and Springborg, J. *Inorg. Chem. 24* (1985) 2129.
7. Bates, R. G. *Determination of pH,* Wiley, New York 1964.
8. Sheldrick, G. M. SHELX-76, Göttingen. *Unpublished.*
9. Cromer, D. T. and Mann, J. B. *Acta Crystallogr., Sect. A 24* (1968) 321.
10. Cromer, D. T. and Liebermann, D. *J. Chem. Phys. 53* (1970) 1891.
11. Stewart, R. F., Davidson, E. R. and Simpson, W. T. *J. Chem. Phys. 42* (1965) 3175.
12. Richens, D. T. and Sykes, A. G. *J. Chem. Soc., Dalton Trans.* (1982) 1621.
13. Buxton, G. V. In: Sykes, A. G., Ed., *Adv. Inorganic Bioinorg. Mechanisms,* Academic Press 1984, Vol. 3, p. 134.
14. *Stability Constants of Metal–Ion Complexes. Part A.* IUPAC Chemical Data Series No. 21, Pergamon Press 1982.
15. Miskowski, V. M., Robbins, J. L., Treitel, I. M. and Gray, H. B. *Inorg. Chem. 14* (1975) 2318.
16. Lever, A. B. P. and Gray, H. B. *Acc. Chem. Res. 11* (1978) 348.
17. Miskowski, V. M., Santasiero, B. D., Schaeffer, W. P., Ansok, G. E. and Gray, H. B. *Inorg. Chem. 23* (1984) 172.
18. Thewalt, U. and Struckmeier, G. *Z. Anorg. Allg. Chem. 419* (1976) 163.
19. Wieghardt, K., Schmidt, W., Nuber, B., Prikner, B. and Weiss, J. *Chem. Ber. 113* (1980) 36.

Received July 15, 1987.